Vol. 212: 53–67, 2001 | MARINE ECOLOGY PROGRESS SERIES
Mar Ecol Prog Ser | Published March 8

Short-term variability of photosynthetic parameters and particulate and dissolved primary production in the Alboran Sea (SW Mediterranean)

Xosé Anxelu G. Morán*, Marta Estrada

Departament de Biologia Marina i Oceanografia, Institut de Ciències del Mar, CSIC, Pg. Joan de Borbó, s/n, 08039 Barcelona, Spain

ABSTRACT: The short-term variability of photosynthesis-irradiance (*P-E*) relationships and integrated primary production at 3 stations (Stns A, B, C in a coastal-offshore gradient) located across the Western Alboran Sea Gyre (SW Mediterranean) were investigated during a High Frequency Flux Experiment (1 to 16 May 1998). Photosynthetic production of total, particulate and dissolved organic carbon (TOC, POC and DOC respectively) was considered separatedly in 34 experiments. Photosynthetic parameters were calculated for TOC and POC data. For POC measurements, maximum photosynthetic rate ($P^B_{m\ POC}$) and the initial slope of the *P-E* curve (α) varied between 0.59 and 6.25 mg C (mg chl *a*)$^{-1}$ h^{-1} and 0.0023 and 0.0182 mg C (mg chl *a*)$^{-1}$ h^{-1} (µmol photons m^{-2} s^{-1})$^{-1}$, respectively, and were significantly correlated, showing a similar decrease with depth. No photoinhibition was detected at any depth and the light saturation parameter (E_k) was on average 251 µmol photons m^{-2} s^{-1}, suggesting that phytoplankton assemblages were acclimated to high irradiance levels in the whole area. Percent extracellular release (PER) obtained for each experimental irradiance (PER_E = DOC/[POC+DOC]) showed an inverse relationship with irradiance when data from all the *P-E* experiments were pooled. A light-saturated chl *a*-normalized DOC production rate ($P^B_{m\ DOC}$) was calculated as $P^B_{m\ TOC} - P^B_{m\ POC}$, and PER_m values calculated as $P^B_{m\ DOC}/P^B_{m\ TOC}$ tended to increase with depth. Integrated particulate and total primary production varied considerably (23- and 35-fold, respectively), but tended to decrease along a coastal-offshore gradient. During the cruise, a subsurface phytoplankton bloom was advected into Stn A, increasing primary production rates up to 1 g C m^{-2} d^{-1}. Average particulate primary production was 632 mg C m^{-2} d^{-1} at Stn A, 388 mg C m^{-2} d^{-1} at Stn B and 330 mg C m^{-2} d^{-1} at Stn C, with dissolved primary production ranging from 4 to 44 % of total values. Integrated primary production was significantly correlated with surface chl *a* but not with integrated chl *a*. This finding has implications for the estimation of regional primary production based on remote sensing of near-surface pigments. Altogether, the results confirmed that the high hydrodynamism of the Alboran Sea was associated with marked biological variability and episodic high primary production events.

KEY WORDS: Phytoplankton · *P-E* relationships · Short-term variability · Primary production · DOC · Upwelling

INTRODUCTION

Over the past few decades, the amount of available data on aquatic photosynthesis has increased enormously. However, detailed studies of its spatio-temporal variability are still needed in order to obtain more accurate estimates of primary productivity in many marine regions. One of the tools for assessing differences in the activity of phytoplankton is the study of photosynthesis-irradiance (*P-E*) relationships. *P-E* curves are widely used for understanding the physiology and ecology of phytoplankton assemblages (e.g. Platt et al. 1980, Sakshaug et al. 1997) and are specially suitable for meso- and basin-scale

*Present address: Instituto Español de Oceanografia, Centro Oceanográfico de Xixón, Camin de L'Arbeyal, s/n, 33212 Xixón, Spain. E-mail: xelu@icm.csic.es

studies because they are less demanding of ship time than other methods. Moreover, the photosynthetic parameters describing the *P-E* relationships are required for the development of models aimed at deriving primary production from remotely sensed near-surface pigments (Platt & Sathyendranath 1988, Longhurst et al. 1995). The lack of information on the spatial and temporal variability of photosynthetic parameters may be a serious constraint for the accuracy of currently used models of primary production in the ocean (Behrenfeld & Falkowski 1997a, Marañón & Holligan 1999). Often, single time data of primary production are taken as representative for extended periods, without information on their variability at shorter time scales.

The Alboran Sea occupies a key geographical position in the Mediterranean and presents an intense hydrodynamism. The water circulation in the Alboran Sea (Minas et al. 1991, Tintoré et al. 1991) is characterized by 2 anticyclonic gyres of ca 100 km in diameter, the Western and Eastern Alboran Sea Gyres, which occupy the respective sub-basins and are easily seen in sea surface temperature satellite images. These quasi-persistent gyres (Heburn & La Violette 1990) are formed by the superficial inflow of Atlantic water which crosses the Strait of Gibraltar and gradually mixes with the resident Mediterranean waters, creating the so-called Modified Atlantic Water (MAW). In the northern part of the Western Alboran Gyre, the frontal zone formed at the boundary of the MAW jet and the saltier (>37.5) Mediterranean waters presents intermittent nutrient upwelling into the upper layers of the water column (Coste et al. 1988, Packard et al. 1988, Perkins et al. 1990, Minas et al. 1991). This upwelling has been associated with enhanced plankton productivity, but very few studies have reported primary production rates. Minas et al. (1991) carried out one of the few attempts to estimate primary production within the Western Alboran Gyre using an approximation based on nitrate consumption over time. The rate of new primary production thus obtained (635 mg C m^{-2} d^{-1}) was slightly higher than the average for other Mediterranean areas (e.g. Sournia 1973, Estrada 1981, Platt 1985, Estrada et al. 1993), but below the expected value for a high productivity site (cf. estimates, within the jet of MAW further east, in Lohrenz et al. 1988b). A number of recent papers have reported elevated biomass of planktonic organisms in the area (e.g. Jiménez et al. 1987, Rodríguez et al. 1994, 1998), but only Fernández et al. (1994) and Videau et al. (1994) included direct measurements of primary production in the Alboran Sea, across the Almería-Oran front in the eastern sub-basin (Tintoré et al. 1991). Due to the episodic nature of the physical forcing in the entire basin, the position of the MAW-Mediterranean water front fluctuates largely at short time scales (Perkins et al. 1990).

This paper presents an investigation of the short-term temporal variations of phytoplanktonic photosynthesis at 3 repeatedly sampled stations, located across the Western Alboran Gyre, during a High Frequency Flux Experiment (HFFE) conducted in May 1998. The aim of the cruise, as part of the European Union MTP-II Project MAss Transfer and Ecosystem Response (MATER), was to study the high frequency processes controlling the pelagic-benthic coupling in the northern part of the gyre. *P-E* relationships were investigated and the derived photosynthetic parameters were used to obtain daily integrated primary production. *P-E* experiments have seldom tried to differentiate between particulate and dissolved primary production (Sakshaug et al. 1997), although the release of dissolved compounds by phytoplankton can significantly contribute to total primary production (Norrman et al. 1995, Biddanda & Benner 1997) and provide substrates readily assimilable by heterotrophic bacteria (Baines & Pace 1991, Amon & Benner 1994). In our *P-E* experiments, we performed direct measurements of the extracellular release of photosynthetic carbon and considered simultaneously total, particulate and dissolved organic carbon (TOC, POC and DOC respectively) production. To our knowledge, only Fernández et al. (1994) had previously dealt with phytoplanktonic DOC release in this marine area. Their conclusion, of a higher contribution of extracellular release to total primary production in the more oligotrophic areas of the Alboran Sea, was addressed during this cruise. In addition, the effect of irradiance on the relative importance of phytoplanktonic DOC production was investigated. To date, systematic studies on the relationships between irradiance and release of photosynthate have been almost exclusively carried out with algal cultures (Verity 1981, Zlotnik & Dubinsky 1989). The *P-E* data set obtained here allowed for an assessment of these relationships for natural phytoplankton assemblages.

MATERIAL AND METHODS

The experiments were conducted during the MTP-II-MATER/HESP/04-98 cruise on board the RV 'Hespérides' from 2 to 13 May 1998. A total of 34 *P-E* experiments (see Table 1 for details) were performed at 3 stations: Stn A (36° 23′ N, 4° 15′ W, 664 m depth), Stn B (36° 14′ N, 4° 15′ W, 984 m depth) and Stn C (36° 0′ N, 4° 15′ W, 1320 m depth), located along a coastal-offshore gradient crossing the northern part of the Western Alboran Gyre (Fig. 1A). The stations were visited 4 times during the cruise and sampled before noon (mostly between 09:00 and 10:00 h GMT). In

addition, an afternoon sample was taken during the first visit to all stations and the fourth visit to Stns A and C. Hereafter, the *n*th visit to Stn X is represented as Stn X*n* (e.g. Stns A1, C4b), with 'b' standing for the afternoon sample.

Optics and hydrography. Vertical profiles of photosynthetically active radiation (PAR, 400 to 700 nm) were obtained immediately after water sampling with a Li-Cor spherical quantum sensor attached to a Seabird 25 CTD system. Vertical light attenuation coefficients (K) were calculated every 10 m, instead of using the whole profile, due to the marked changes of slope of the log-transformed data versus depth. Incident irradiance was continuously measured with a pyranometer connected to a Li-Cor LI-1000 data logger. A Neil Brown Mark III CTD was used to obtain vertical profiles of temperature, salinity and density. The depth of the upper mixed layer (Z_{uml}) was determined as the depth where the change in density (σ_t) was ≥ 0.05 kg m^{-3} over a 5 m depth interval (Mitchell & Holm-Hansen 1991). Water samples for nutrient and biological determinations were collected at 10 to 11 discrete depths with 12 l Niskin bottles from a rosette sampler attached to the CTD. Samples for nutrient analysis were immediately frozen and concentrations of nitrate, nitrite, phosphate and silicate were determined on unfiltered samples in the laboratory with a Technicon autoanalyzer.

Chlorophyll *a* (chl *a*) concentration. For the determination of total chl *a* concentration, samples of 100 ml were filtered onto Whatman GF/F filters. In most experiments, size-fractionation of chl *a* (<20, >5 and <2 µm) was also carried out. Detailed information on methods and results will be given in Arin et al. (unpubl.). All filters were 25 mm in diameter and differential pressures were kept below 200 mm Hg. Pigments were extracted in acetone for 24 h in the dark at 4°C prior to fluorescence measurement without acidification with a Turner Designs fluorometer (Yentsch & Menzel 1963). Calibration was made comparing the fluorescence readings with measurements of chl *a* concentration carried out with a spectrophotometer.

***P-E* relationships.** At each station, water was taken from 2 depths, chosen to represent the upper mixed layer ('surface' samples), and the deep chlorophyll maximum (DCM) if present, or the part of the euphotic zone located below the pycnocline ('deep' samples). Sometimes, the upper mixed layer was deeper than the photic zone (e.g. Stn C3) and the deep sample was chosen at an arbitrarily intermediate depth. The DCM was located between 20 and 50 m depth. Fourteen light and 1 dark (covered with aluminium foil) sterile polystyrene tissue culture bottles (Corning) containing 70 ml water samples were incubated for each experiment and depth, in closed linear incubators with circulating water at the *in situ* sampling temperature (±0.5°C). Before starting the experiments, all bottles were spiked with 6.37 to 9.31 µCi (2.36 to 3.44 × 10^5 Bq) of ^{14}C-bicarbonate (The International Agency for ^{14}C Determination, VKI, Denmark). Incubations lasted for ca 2 to 3 h. Illumination was provided by Phillips halogen lamps (50 W). The irradiance level at each position was directly measured with an Illuminova (Sweden) spherical PAR light-sensor placed inside a bottle. An intercalibration with a spherical Li-Cor quantum sensor proved that both sensors gave similar values. Values ranged from 5.4 to 1515 µmol photons m^{-2} s^{-1} for the incubator with the more superficial samples, and from 8.5 to 880 µmol photons m^{-2} s^{-1} for the incubator with the deeper ones. The desired attenuation of the irradiance received by the bottles was achieved by using several neutral density filters.

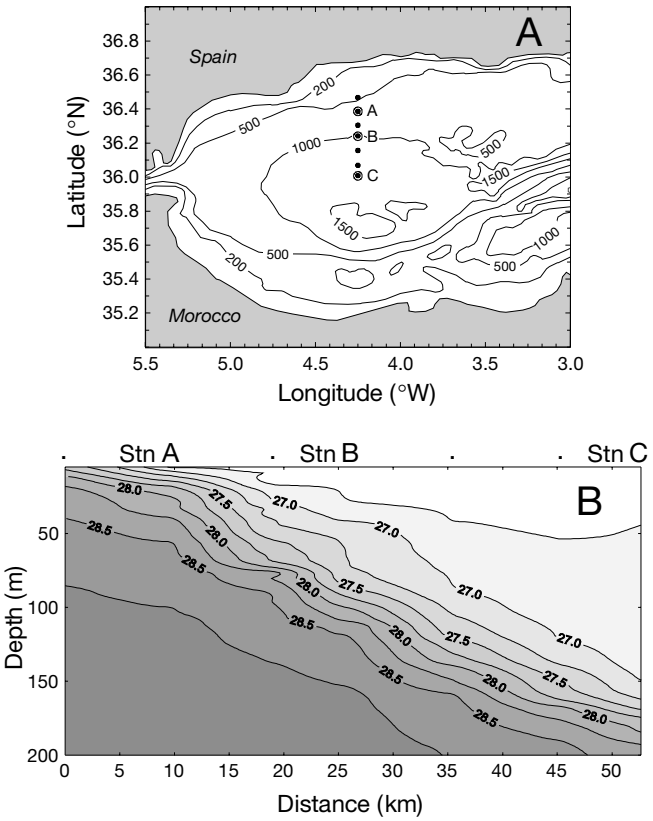

Fig. 1. (A) Location of the 3 repeatedly sampled Stns A, B and C and the stations of the transect shown in (B). (B) Distribution of density (σ_t, kg m^{-3}) along the transect carried out between 10 and 11 May 1998

At the end of the incubation, subsamples were taken for determination of labelled TOC, POC and DOC, except at Stns A2, B2 and C2, in which only TOC and POC were measured. DOC was defined as the fraction passing a Millipore GSWP 0.22 µm filter (mixed cellulose esters, 25 mm in diameter). Subsamples of 5 ml

each were taken for TOC and DOC. The remaining 60 ml were filtered onto another 0.22 µm filter for determination of labelled POC. The vacuum pressure was always kept below 80 mm Hg. Labelled DOC in the water sample was considered as 'dissolved primary production' originating from phytoplanktonic photosynthetic activity, but it may derive not only from dissolved organic matter released by phytoplankton but also from protozoan sloppy feeding or cellular lysis (Nagata 2000). The measurement of labelled DOC at the end of the incubation can cause an underestimation of the total phytoplanktonic DOC production if heterotrophic bacteria are simultaneously removing it. Therefore, the estimated DOC production rate should be considered as a minimum approximation. This procedure implicitly assumes linear increase in labelled DOC during the incubation period (Lancelot 1979, Morán et al. in press). The time elapsed before observing a departure from linearity during a ^{14}C primary production experiment has been shown to be very variable (e.g. from minutes to hours, Lancelot 1979, Coveney 1982), but based on previous experiments in the NW Mediterranean (Morán & Estrada unpubl. data) linearity could be assured for a minimum period of 2 h. In any case, we assumed that the potential underestimation did not mask the general trends in calculated DOC production rates.

Filters were fumed with concentrated HCl for ca 12 h, and TOC and DOC samples were acidified with 1 ml HCl 1 M and left open in an orbital shaker for at least 6 h in order to remove inorganic ^{14}C. This time span has proven sufficient to eliminate inorganic label in previous tests. Radioactivity was measured in a Beckman LS6000 (LL) liquid scintillation counter, and disintegrations min^{-1} (dpm) were calculated with the external standard method. Before further calculations, dark bottle values of labelled TOC, POC and DOC were subtracted from the light bottle values for correction of non-photosynthetic uptake of carbon. Dark bottle values were on average 74 ± 31 SD dpm for $PO^{14}C$, 71 ± 11 dpm for $TO^{14}C$ and 82 ± 16 dpm for $DO^{14}C$. When considering all the experiments, dpm for samples incubated in the light were on average 231 ± 185 % SD higher than the corresponding dark value for TOC, and 28 ± 15 % higher for DOC. These differences between light and dark bottles were significant (paired *t*-test for experimental means: $p < 0.00001$; $n = 34$ for TOC; $p = 0.0008$, $n = 28$ for DOC).

POC and TOC measurements were initially fitted to the exponential model of Platt et al. (1980) using non-linear least-squares regression (KaleidaGraph software):

$$P^B = P^B_s [1 - \exp(-\alpha E/P^B_s)] [\exp(-\beta E/P^B_s)]$$

where P^B [mg C (mg chl *a*)$^{-1}$ h^{-1}] is the chl *a*-normalized photosynthetic rate, P^B_s [mg C (mg chl *a*)$^{-1}$ h^{-1}] is the maximum chl *a*-normalized photosynthetic rate without photoinhibition, α [mg C (mg chl *a*)$^{-1}$ h^{-1} (µmol photons m^{-2} s^{-1})$^{-1}$] is the initial slope of the *P-E* curve and β (same units as α) is the photoinhibition parameter. As fitted β values were 0 in all cases (see 'Results'), P^B_s in Platt et al.'s model was equivalent to P^B_m in the model proposed by Webb et al. (1974):

Table 1. Sampling dates, times and depths of the *P-E* experiments. Also shown are the depths of the upper mixed layer (Z_{uml}), the euphotic zone (Z 1 % E_0) and the nutricline for nitrate ($Z\,NO_3$) and phosphate ($Z\,PO_4$), and the mean irradiance within the upper mixed later (E_{uml}). Details explained in the text. –: not determined. Low E_{uml} values for Stns C3, C4 and C4b were largely due to cloudy conditions

Stn	Date (1998)	Time (GMT)	Depth (m)	Z_{uml} (m)	Z 1 % E_0 (m)	$Z\,NO_3$ (m)	$Z\,PO_4$ (m)	E_{uml} (µmol photons m^{-2} s^{-1})
A1	2 May	09:40	5, 63	35	54	26	31	229
A1b	2 May	16.25	30, 80	33	–	–	–	–
B1	3 May	09:08	5, 35	36	53	51	150	149
B1b	3 May	16:50	30, 80	34	–	–	–	–
C1	4 May	10:00	5, 80	65	51	72	68	162
C1b	4 May	16:10	30, 80	63	–	–	–	–
A2	5 May	09:30	25, 50	31	43	<5	<5	235
B2	6 May	09:40	25, 50	29	50	5	<5	271
C2	7 May	09:05	35, 50	11	49	115	126	442
A3	8 May	11:50	15, 50	9	35	7	12	423
B3	9 May	09:40	25, 50	14	61	43	53	318
C3	10 May	08:10	5, 55	133	56	105	149	37
A4	11 May	08:00	5, 45	7	42	<5	6	220
A4b	11 May	16:18	5, 40	5	39	–	–	282
B4	12 May	08:40	5, 25	9	55	8	5	459
C4	13 May	10:15	5, 50	32	58	71	80	31
C4b	13 May	15:05	5, 35	12	63	–	–	54

$$P^B = P^B_m [1 - \exp(-\alpha E / P^B_m)]$$

where P^B_m [mg C (mg chl *a*)$^{-1}$ h^{-1}] is the maximum chl *a*-normalized photosynthetic rate. The saturating irradiance or light saturation parameter (E_k) was estimated as P^B_m/α.

Once P^B_m was calculated for TOC and POC data ($P^B_{m\ TOC}$, $P^B_{m\ POC}$), a light-saturated chl *a*-normalized photosynthetic rate for the dissolved fraction ($P^B_{m\ DOC}$) was calculated as

$$P^B_{m\ DOC} = P^B_{m\ TOC} - P^B_{m\ POC}$$

Integrated primary production. The *P-E* parameters (P^B_m, α), together with the depth profiles of PAR and chl *a* down to 100 m depth, and the hourly irradiance, were used to estimate the daily integrated primary production, both the total ($PP_{int\ TOC}$) and the particulate ($PP_{int\ POC}$), with the trapezoidal method. Two procedures of integration (no. 1 and no. 2) were applied to POC- and TOC-derived photosynthetic parameters. In procedure no. 1, the *P-E* parameters of the most superficial sample were assumed to be representative of the phytoplankton assemblages of the upper layer down to the beginning of the DCM, and those from the DCM were in turn assumed to be representative of the phytoplankton assemblages of the rest of the water column, down to 100 m. A discrete cut-off between both situations was made by visually estimating the depth of the steepest change in the chl *a* profile. In procedure no. 2, P^B_m and α were interpolated by linear regression between the surface and deep values, to estimate values at all the depths where chl *a* was measured.

Statistical analyses other than *P-E* curve fitting were performed with the Statistica software package. Data of chl *a* and PP_{int} were log-transformed to attain normality and homogeneity of variances.

RESULTS

Optics and hydrography

The mean total daily incident irradiance during the cruise was 35.4 mol photons m^{-2} d^{-1} (range 10.1 to 49.6). The vertical light attenuation coefficients (K) for all 10 m depth intervals ranged from 0.047 to 0.237 m^{-1}. Using these K values, the depth of the euphotic layer (Z 1 % E_0, i.e. the depth with 1 % of the irradiance level at the surface) was estimated (Table 1). Average values were 44 ± 8 m SD at Stn A, 55 ± 5 m at Stn B and 54 ± 4 m at Stn C. The mean daily irradiance in the upper mixed layer (see below) was generally well above 100 µmol photons m^{-2} d^{-1} for all the experiments performed at Stns A and B, but less than 50 µmol photons m^{-2} d^{-1} for the experiments at Stns C3, C4 and C4b (Table 1).

The depth profiles of temperature, salinity and density for visits 1 through 4 to the 3 stations are shown in Fig. 2. A temporal trend towards a shoaling of the upper mixed layer (Z_{uml}) was observed for the consecutive vis-

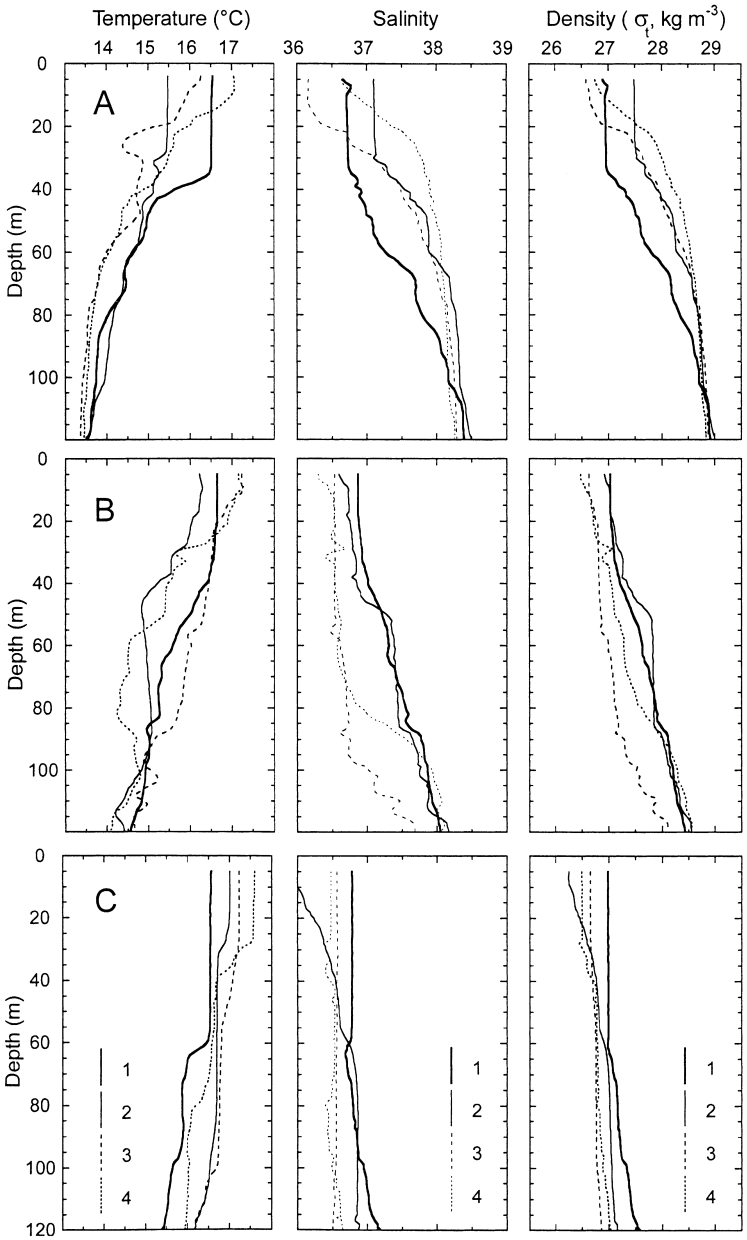

Fig. 2. Depth profiles of temperature, salinity and density for visits 1–4 to Stns A, B and C

its to Stns A and B. No trend was observed for Stn C, in which the mixed layer was generally deeper than at the other 2 stations (Table 1). Values of Z_{uml} at Stns A and B showed averages of 21 ± 15 and 22 ± 13 m, respectively. A northward shallowing of the isopycnals along the transect of the 3 stations was very apparent (Fig. 1B), reflecting the position of the front formed by the jet of MAW and the coastal Mediterranean waters.

The depths of the nutriclines of nitrate ($Z\,NO_3$, first depth with concentration ≥1 µM) and phosphate ($Z\,PO_4$, first depth with concentration ≥0.1 µM) are shown in Table 1. During the cruise, an upwelling event produced a notable shallowing of both nutriclines at Stn A: $Z\,NO_3$ and $Z\,PO_4$ decreased from, respectively, 26 and 31 m at Stn A1 to <5 m at Stn A2. At Stn A3 a marked decrease of the concentration of nitrate, phosphate and silicate was found coinciding with the depth of a conspicuous DCM (see below). Nutrient injection into the upper layers of Stn B2 was also recorded (Table 1), but with apparently no effect on the buildup of algal biomass. Nutrient changes at Stn C were much less marked and both nutriclines were always deeper than 70 m.

Chlorophyll *a*

The vertical distribution of chl *a* is shown in Fig. 3. A marked increase in the chl *a* concentration at Stn A was observed from visits 1 through 3, as a likely consequence of the upwelling event commented above. This station presented chl *a* maxima well above 5 mg m^{-3} at around 40 m on the last 2 visits. Maximum values at Stn B (ca 1 mg chl *a* m^{-3}) were generally found at shallow depths (<40 m), although a second deep (>100 m) peak was observed at Stn B4. At Stn C, which presented less variability than the other 2 stations, concentrations were generally below 1 mg chl *a* m^{-3}, with a decreasing trend between visits 1 and 4.

Integrated chl *a* values down to 100 m depth (chl a_{int}) ranged from 36 to 307 mg chl *a* m^{-2}. Mean values for the 3 stations were 170 ± 117 SD (Stn A), 49 ± 13 (Stn B) and 58 ± 17 (Stn C) mg chl *a* m^{-2}. The concentration of chl *a* at the surface (chl a_0) was significantly correlated to chl a_{int} (log-log, r = 0.60; p = 0.023; n = 14). The depth of the euphotic layer (Z 1% E_0) showed significant negative correlations with chl a_{int}, chl a_0 and the measured fractions of chl *a* for all available data, indicating a high contribution of phytoplankton biomass to the vertical light attenuation coefficients. The most remarkable temporal changes were again observed at Stn A, where chl a_{int} at Stns A3 and A4 were respectively 4.8 and 3.6 times higher than the initially sampled (Stn A1) value. At this station, significant high negative correlations were found between Z_{uml} and chl a_{int}, for total values (r = −0.98; p = 0.004; n = 5) and the fractions >5 µm (r = −0.99; p = 0.009; n = 4) and >20 µm (r = −0.97; p = 0.026; n = 4), indicating the effect of the upwelling on the buildup of algal biomass. Changes in the dominant organisms and the percentage of the different size-classes of chl *a* confirmed the appearance of an advected phytoplankton bloom at Stn A. Between visits 1 and 4 at Stn A, a shift in dominance from coccolithophorids and autotrophic flagellates to diatoms occurred (L. Arin pers. comm.) and whereas the percentage of chl a_{int} >20 µm decreased steadily throughout the visits to Stns B and C to a final value of 9 and 5% of the total, respectively, such percentage increased from 32% at Stn A1 to 60% at Stn A3 (54% at Stn A4). The depth of the nutriclines, as a proxy for nutrient supply into the upper layer (Cleveland et al. 1989), was significantly correlated with chl a_0 for all stations (r = −0.59, p = 0.042 for $Z\,NO_3$; r = −0.63, p = 0.028 for $Z\,PO_4$; n = 12).

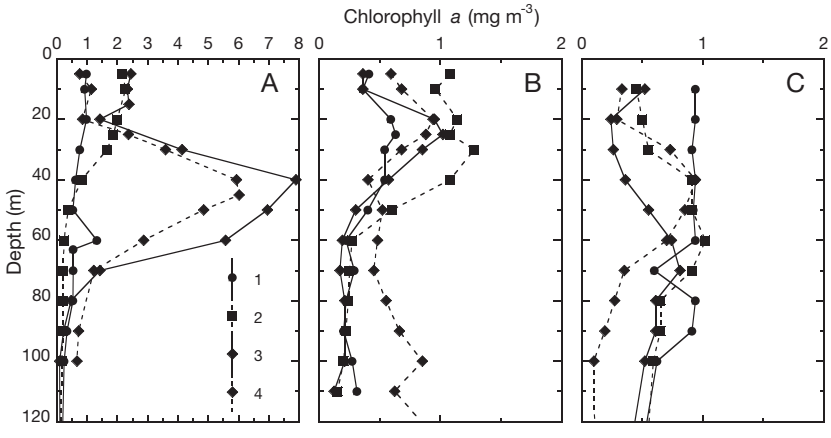

Fig. 3. Vertical distribution of total chl *a* for visits 1–4 to Stns A, B and C. Note the different scale for Stn A

Photosynthetic parameters

Selected *P-E* curves obtained from POC data are shown in Fig. 4. Whereas $PO^{14}C$ and $TO^{14}C$ similarly increased in a typical non-linear fashion within the experimental range of irradiance, $DO^{14}C$ virtually did not change. To test this, average DOC was calculated at each experiment for all irradiance levels lower and greater than the corresponding saturating irradiance (E_k). The difference between both sets of values was not significant (Wilcoxon's matched pairs test, p = 0.56; n = 28). Table 2 shows the mean photosynthetic parameters

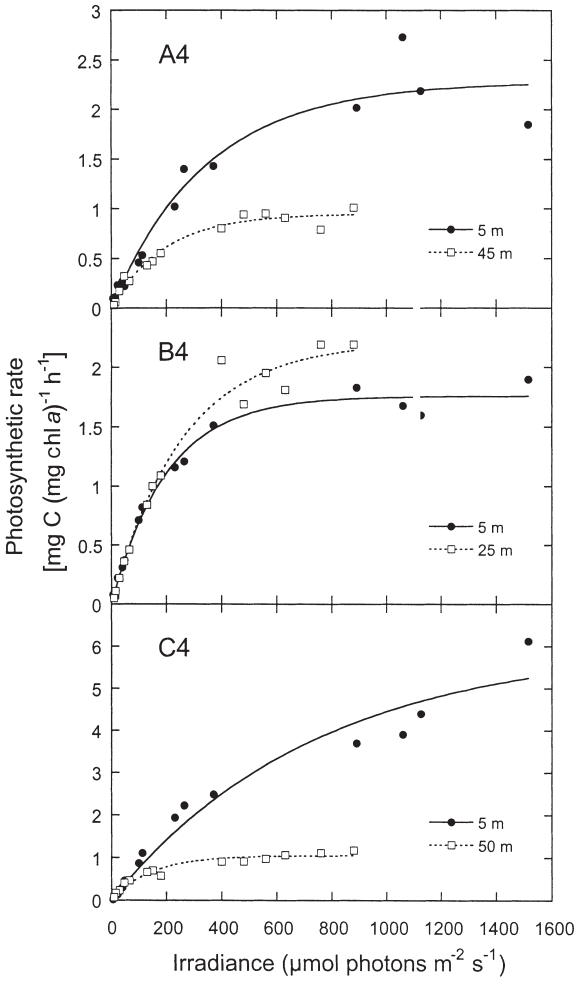

Fig. 4. Photosynthesis-irradiance plots and fitted curves for the experiments carried out at Stns A4, B4 and C4

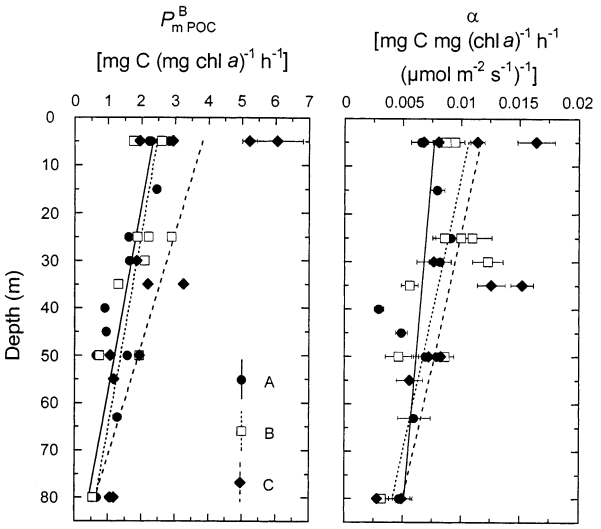

Fig. 5. Distribution of $P^B_{m\ POC}$ and α with depth for the *P-E* experiments. Bars are standard errors of the estimates. Lines are linear regressions for each station. Coefficients of correlation for $P^B_{m\ POC}$: r = –0.86, p = 0.0003 (Stn A); r = –0.73, p = 0.017 (Stn B); r = –0.72, p = 0.008 (Stn C). Coefficients of correlation for α: r = –0.46, p = 0.13 (Stn A); r = –0.68, p = 0.031 (Stn B); r = –0.60, p = 0.041 (Stn C)

calculated with POC data for the depth ranges less than and greater than 30 m. Of the 34 curves obtained, 28 yielded good fits to the model with $r^2 > 0.90$ and the remaining 6 had fits with r^2 between 0.80 and 0.90. Both the maximum chl *a*-normalized photosynthetic rate ($P^B_{m\ POC}$) and the maximum light utilization coefficient (α) ranged over 1 order of magnitude, from 0.54 to 6.05 mg C (mg chl *a*)$^{-1}$ h^{-1} and from 0.0028 to 0.0168 mg C (mg chl *a*)$^{-1}$ h^{-1} (µmol photons m^{-2} s^{-1})$^{-1}$, respectively. Highest values of both parameters were found in surface waters of Stns C4 and C4b. No photoinhibition was detected with the experimental irradiance range, even for the deepest samples (80 m), and the values of E_k were generally above 100 µmol photons m^{-2} s^{-1} (average 251 ± 111 SD µmol photons m^{-2} s^{-1}) regardless of the sampling depth. Both $P^B_{m\ POC}$ and α were significantly negatively correlated with depth at the 3 stations (Fig. 5). Despite noticeable changes in chl *a* concentration, especially at Stn A, surface photosynthetic parameters varied little throughout the cruise, except for Stn C, where $P^B_{m\ POC}$ increased from values similar to those of Stns A and B [2 to 3 mg C (mg chl *a*)$^{-1}$ h^{-1}] to ca 6 mg C (mg chl *a*)$^{-1}$ h^{-1} on the last visit. With pooled data from all experiments, $P^B_{m\ POC}$ and α were significantly correlated (Fig. 6). The linear regression between both parameters was $P^B_{m\ POC} = -0.09 + 244\alpha$; $p < 0.000001$; $r^2 = 0.69$; n = 33.

The slope of the regression between P^B_m and α, another way of estimating the average E_k, gave a value

Table 2. Mean values ± SD of photosynthetic parameters calculated with POC measurements in the depth ranges 0 to 30 and >30 m for each station. $P^B_{m\ POC}$: maximum chl *a*-normalized photosynthetic rate [mg C (mg chl *a*)$^{-1}$ h^{-1}]; α: initial slope of the *P-E* curve [mg C (mg chl *a*)$^{-1}$ h^{-1} (µmol photons m^{-2} s^{-1})$^{-1}$]; E_k: light saturation parameter (µmol photons m^{-2} s^{-1}). Chl *a*: concentration of total chl *a* (mg m^{-3}) weighted for the depths 0 to 30 and 30 to 80 m

Stn	Depth (m)	Chl *a*	$P^B_{m\ POC}$	α	E_k
A	0–30	1.70 ± 0.68	2.18 ± 0.47	0.0078 ± 0.0010	285 ± 76
	>30	1.49 ± 1.33	1.00 ± 0.36	0.0056 ± 0.0018	191 ± 72
B	0–30	0.75 ± 0.25	2.24 ± 0.43	0.0100 ± 0.0014	227 ± 53
	>30	0.39 ± 0.25	1.13 ± 0.63	0.0055 ± 0.0023	211 ± 60
C	0–30	0.56 ± 0.27	3.60 ± 1.93	0.0101 ± 0.0040	372 ± 214
	>30	0.45 ± 0.08	1.59 ± 0.83	0.0081 ± 0.0044	228 ± 74

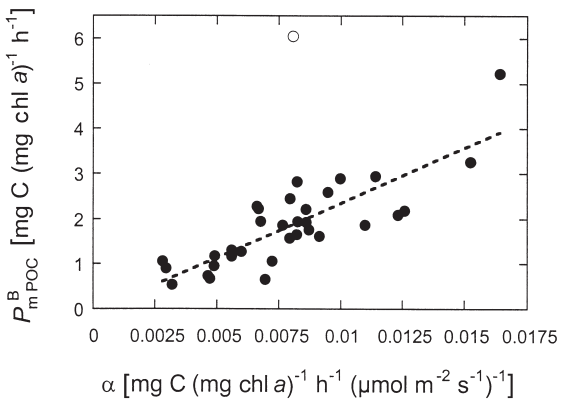

Fig. 6. Relationship between $P^B_{m\ POC}$ and α for all experiments. Linear regression equation given in the text. The open symbol (Stn C4) was not included in the calculations

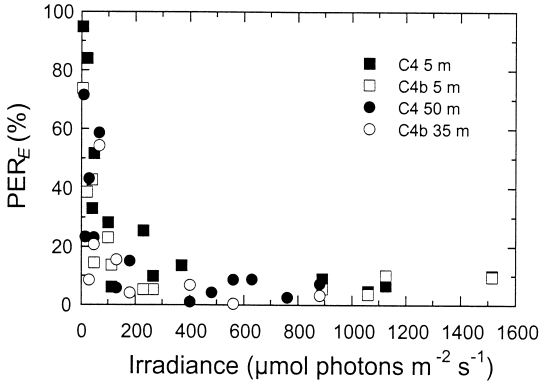

Fig. 7. Relationship between percent extracellular release (PER$_E$) and irradiance in the *P-E* experiments carried out with samples from different depths at Stns C4 and C4b

of 244 µmol photons m^{-2} s^{-1} (cf. 251 µmol photons m^{-2} s^{-1}). Photosynthetic parameters were not correlated with the amount of chl *a* in the different size-classes or with nutrient concentrations, except for nitrite, which was negatively correlated with P^B_m (–0.48, p = 0.017, n = 24) and E_k (–0.46, p = 0.026, n = 24), probably reflecting an opposite variation with depth.

Mean *P-E* parameters calculated with TOC measurements are given in Table 3. r^2 values for the fitted model were generally lower and more variable than for POC measurements. Paired *t*-tests were performed to compare P^B_m, α and E_k values obtained with TOC and POC measurements. P^B_m values obtained with TOC ($P^B_{m\ TOC}$) were significantly higher than corresponding $P^B_{m\ POC}$ values (p = 0.0027, n = 34). Differences were not significant for α values (p = 0.67, n = 34) and marginally significant for E_k (p = 0.047, n = 34).

Particulate and dissolved primary production

Percent extracellular release (PER) values were obtained for each experimental irradiance (PER$_E$) by calculating DOC/(POC + DOC) from the direct measurements of both variables. As an example, Fig. 7 shows the variation of PER$_E$ with incubation irradiance for the *P-E* experiments carried out at Stns C4 and C4b. Increased values of PER$_E$ were obtained at low irradiances, whereas for irradiances >200 µmol photons m^{-2} s^{-1}, PER$_E$ was generally below 15%. Although greatly variable, the trend of increasing PER$_E$ with decreasing irradiance was still observed with all available data, both for the experiments under the surface and the deep ranges of irradiance (Fig. 8).

Table 3. Photosynthetic parameters calculated with TOC measurements (see Table 2 for details)

Stn	Depth (m)	$P^B_{m\ TOC}$	α	E_k
A	0–30	2.78 ± 0.94	0.0079 ± 0.0027	377 ± 117
	>30	1.50 ± 0.66	0.0052 ± 0.0032	393 ± 342
B	0–30	2.68 ± 0.32	0.0090 ± 0.0021	319 ± 119
	>30	1.57 ± 1.13	0.0062 ± 0.0030	255 ± 120
C	0–30	3.90 ± 1.95	0.0110 ± 0.0042	362 ± 166
	>30	1.77 ± 0.72	0.0091 ± 0.0039	210 ± 70

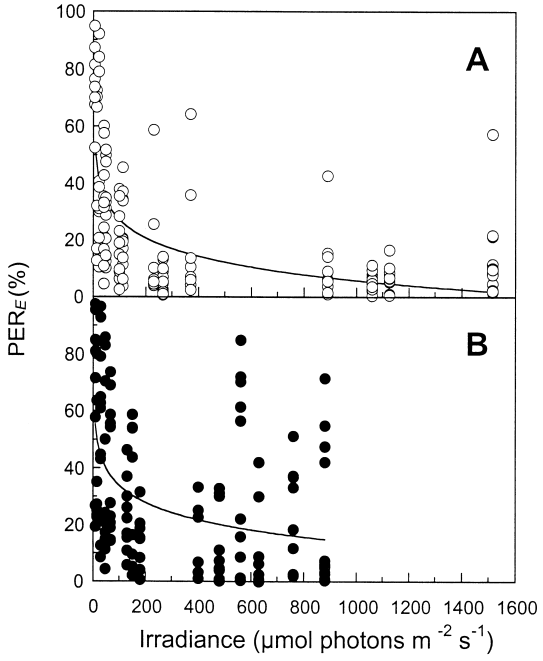

Fig. 8. Relationships between PER$_E$ and irradiance (*E*) for all experiments. (A) Superficial samples (experiments made under a range of 5.4 to 1515 µmol photons m^{-2} s^{-1}). Regression line: PER$_E$ = 71.6 – 22.1 log*E*; p = 0.000001, r^2 = 0.46; n = 146. (B) Deep samples (experiments made under a range of 8.5 to 880 µmol photons m^{-2} s^{-1}). Regression line: PER$_E$ = 74.1 – 20.1 log*E*; p < 0.000001, r^2 = 0.22; n = 134

In 23 out of the 34 experiments, the difference between $P^B_{m\ TOC}$ and $P^B_{m\ POC}$ was positive and a light-saturated chl *a*-normalized photosynthetic rate for the dissolved fraction ($P^B_{m\ DOC}$) could be calculated as $P^B_{m\ DOC} = P^B_{m\ TOC} - P^B_{m\ POC}$. In the remaining 11 incubations, $P^B_{m\ TOC}$ values were slightly lower than the corresponding $P^B_{m\ POC}$ ones. PER considering these $P^B_{m\ DOC}$ values ($PER_m = P^B_{m\ DOC}/P^B_{m\ TOC}$) tended to increase with depth. A linear regression with all data gave $PER_m = 15 + 0.34Z$; $p = 0.041$; $r^2 = 0.18$; $n = 23$.

Integrated primary production. Relationships with chl *a* concentration

PP_{int} varied noticeably during the cruise at the 3 stations and was also dependent on the procedure used for integration (see Table 4), although to a relatively small extent, as differences were not significant (*t*-test for dependent samples, $PP_{int\ POC}$ no. 1 and $PP_{int\ POC}$ no. 2, $p = 0.14$; $PP_{int\ TOC}$ no. 1 and $PP_{int\ TOC}$ no.2, $p = 0.25$; $n = 14$). Therefore, only the linear interpolation approach values (procedure no. 2) will be used hereafter. $PP_{int\ POC}$ ranged from 42 to 956 mg C m^{-2} d^{-1} and $PP_{int\ TOC}$ ranged from 47 to 1634 mg C m^{-2} d^{-1}. As the effect of phytoplanktonic respiration of labelled carbon in short incubations is low (Williams et al. 1996) and the calculation did not consider phytoplankton respiration during the night, these values would be closer to gross than to net primary production rates (Williams 1993). In general, PP_{int} decreased following the coastal-offshore gradient. Mean (±SE) $PP_{int\ POC}$ values were 632 ± 184 mg C m^{-2} d^{-1} at Stn A, 388 ± 123 mg C m^{-2} d^{-1} at Stn B and 330 ± 149 mg C m^{-2} d^{-1} at Stn C. Except for the first visit, PP_{int} was always highest at Stn A. Due to upwelling and the subsequent nutrient consumption and biomass increase found at this station, PP_{int} increased more than 2-fold from Stns A1 to A2 and A3 (Table 4). During the fourth visit, Stns A and C were sampled twice. From morning to afternoon (ca 8 and 6 h difference, respectively), estimated $PP_{int\ POC}$ increased 1.7-fold at Stn A and 3.0-fold at Stn C. This increase also held true for $PP_{int\ TOC}$, with a 1.9-fold increase at Stn A and 3.0-fold at Stn C.

Particulate and total PP_{int} were well correlated with chl a_0, but not with chl a_{int} ($p > 0.12$). The corresponding linear regressions with chl a_0 (Fig. 9) were: $\log PP_{int\ POC} = 2.63 + 1.11 \log$ chl a_0; $r^2 = 0.55$; $p = 0.0024$; $n = 14$. $\log PP_{int\ TOC} = 2.64 + 1.22 \log$ chl a_0; $r^2 = 0.63$; $p = 0.0007$; $n = 14$.

$PP_{int\ POC}$ was positively correlated to total incident irradiance ($r = 0.65$, $p = 0.011$, $n = 14$) and negatively correlated with the depth of the euphotic layer, Z 1 % E_0 ($r = -0.61$, $p = 0.022$, $n = 14$). This latter negative relationship was expected from the fact that chl absorbs a higher percentage of light, relative to the water, when contained in a narrow layer within a shallow euphotic zone, than when found at deeper levels. As can be seen in Fig. 10, particulate primary production at the 3 stations was mainly confined to the upper layers of the water column. Values >10 mg C m^{-3} d^{-1} were usually only found at depths shallower than 20 m.

Table 4. Estimates of daily integrated particulate ($PP_{int\ POC}$) and total ($PP_{int\ TOC}$) primary production down to 100 m depth obtained with 2 procedures: no. 1, assuming 2 sets of constant P^B_m and α values throughout the water column, changed at the indicated depth; no. 2, using linear regressions for P^B_m and α between the surface and deep values of each experiment. Percent extracellular release for the 0 to 100 m depth range (PER_{int}) is also included (PER_{int} was calculated as [$PP_{int\ TOC}$ no. 2 – $PP_{int\ POC}$ no. 2]/$PP_{int\ TOC}$ no. 2). Mean and standard error (SE) were calculated for Stns 1 to 4 (Stn 4b not included). –: $PP_{int\ POC}$ no. 2 > $PP_{int\ TOC}$ no. 2

Stn	Depth of change (m)	$PP_{int\ POC}$ no. 1	$PP_{int\ POC}$ no. 2	$PP_{int\ TOC}$ no. 1	$PP_{int\ TOC}$ no. 2	PER_{int} (%)
			(mg C m^{-2} d^{-1})			
A1	60	474	455	587	584	22
A2	40	729	920	1184	1633	44
A3	30	918	956	898	997	4
A4	30	199	198	150	149	–
A4b	30	354	345	282	277	–
A mean		580	632	705	841	24
SE		156	184	222	316	11
B1	20	203	215	197	200	–
B2	50	638	717	547	482[a]	–
B3	50	238	275	261	314	13
B4	20	191	191[a]	214	210[a]	9
B mean		358	388	322	318	11
SE		107	124	82	66	1
C1	70	656	607	611	559	–
C2	50	385	567	287	415	–
C3	40	105	104	117	117	11
C4	30	43	42	48	47	10
C4b	30	133	126	147	140	10
C mean		297	330	266	284	11
SE		141	149	126	121	0

[a]P^B_m deep value was higher than the surface one, so 2 linear regressions were used: one from the surface to the deep value (with the corresponding positive slope), and one from that depth downwards (with the average negative slope for all available P^B_m data at that Stn)

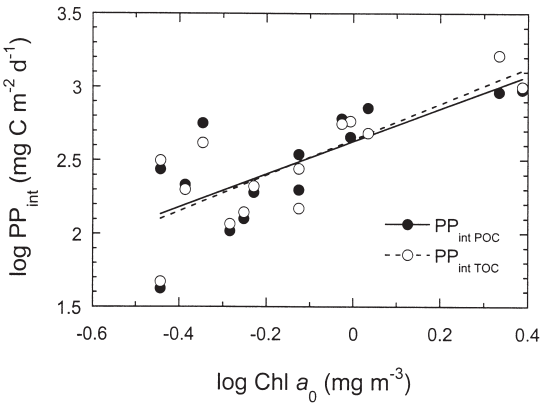

Fig. 9. Relationship between integrated primary production (PP_{int}) and surface chl *a* (chl a_0) for all data. Regression equations are given in the text

An integrated value of PER for the 0 to 100 depth range (PER_{int}) was calculated where possible by using the difference between $PP_{int\ TOC}$ and $PP_{int\ POC}$ as an estimate of the integrated dissolved primary production. These values are shown in Table 4 and were on average higher (24%) at Stn A, although highly variable on different days. At the other 2 stations, average PER_{int} were the same (11%) and virtually constant.

DISCUSSION

Elevated concentrations of chl *a* have been previously reported for the Western Alboran Sea (Jiménez et al. 1987, Minas et al. 1991, Rodríguez et al. 1994, 1998), but direct measurements of primary productivity for this sub-basin are lacking. Our results show that a noticeable variability in chl *a* distribution and primary production rates estimated from *P-E* relationships occurred at a time scale of days in the northern part of the Western Alboran Gyre. The main change observed was a marked increase in phytoplankton biomass and production parallel to nutrient consumption at subsurface levels of Stn A, located in the frontal region between the MAW jet and the Mediterranean waters. At the same time, a shift in the dominant size-classes of chl *a*, from 68% of chl a_{int} smaller than 20 µm to 54% greater than that size, reflected a marked increase in diatom abundance (L. Arin et al. unpubl.). These changes were too fast to have originated *in situ* and can be explained as the result of advection of water masses being affected by an upwelling event of increasing intensity. According to the hydrodynamical regime in the study area, and the location of Stn A in the northern part of the Western Alboran Gyre, the advected waters were probably coming from the west (Gómez et al. 2000).

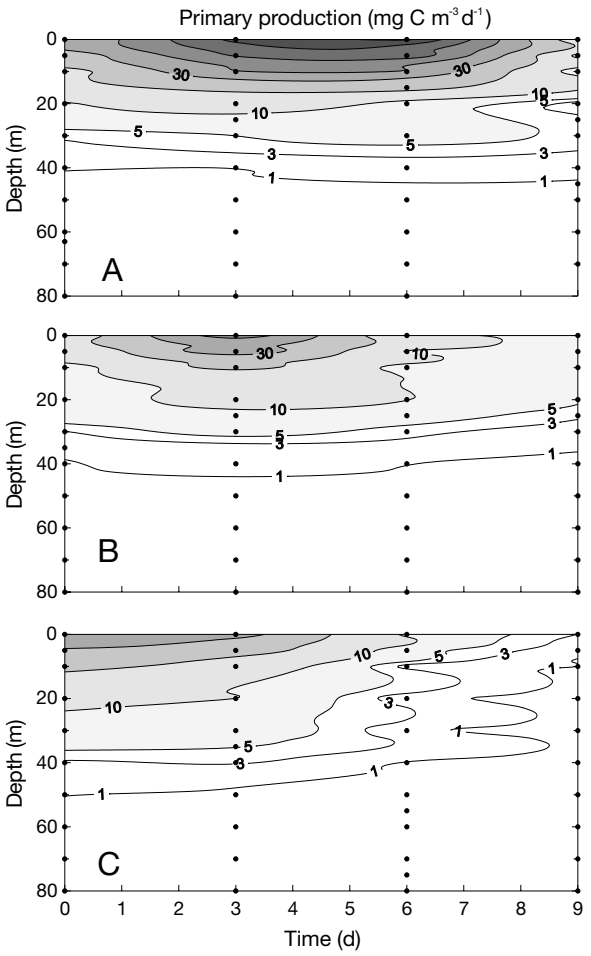

Fig. 10. Temporal variation of the rate of particulate primary production at the 3 sampled stations

Photosynthetic parameters

The range of variation of the maximum photosynthetic rates, with averages of 2.0 ($P^B_{m\ POC}$) and 2.4 mg C (mg chl *a*)$^{-1}$ h^{-1} ($P^B_{m\ TOC}$), was comparable, although shifted to slightly higher values, to that of the unique *P-E* measurements previously reported for the Alboran Sea, at the Almería-Oran Front (Videau et al. 1994). Both $P^B_{m\ POC}$ and $P^B_{m\ TOC}$ varied by a factor of 11 (CV 60%), which was notably high for a small area and short time scale when compared to the variability found during ocean-scale surveys (a factor of 4 in Hood 1995, 9 and 18 in Kyewalyanga et al. 1998, but 30 in Marañón & Holligan 1999) or with a temporally more extended data set (a factor of 4, over a period of 70 d in Côté & Platt 1983). The values of the initial slope or maximum light utilization coefficient (α) were very low [mostly <0.01 mg C (mg chl *a*)$^{-1}$ h^{-1} (µmol photons m^{-2} s^{-1})$^{-1}$, Tables 2 & 3], falling in the lower part of recently reported ranges

covering much larger distances in the Atlantic (Hood 1995, Kyewalyanga et al. 1998, Marañón & Holligan 1999), and varied by a factor of 6. The comparatively lower variability of α compared with P^B_m may have been expected (Geider 1993), as this parameter appears to be a function of basic photochemical reactions (Côté & Platt 1983). The marked increase in P^B_m and α at the surface of Stn C from the first to the last visit (see Fig. 5) suggests that either a shift in the composition of the superficial phytoplankton assemblages or a change in their photophysiological status had occurred. The same water mass was sampled at Stns C4 and C4b as judged from the distribution of physical variables, so the 2-fold increase in α from morning to afternoon [0.008 and 0.016 mg C mg chl a^{-1} h^{-1} (µmol photons m^{-2} $s^{-1})^{-1}$, Fig. 6] could perhaps reflect a process of photoacclimation of the phytoplankton taking place at that time. On the contrary, no trend was observed in the photosynthetic parameters of Stn A during the period of study as a result of the nutrient injection event, even though a change in the hydrological conditions and the dominant phytoplankton assemblages had effectively taken place.

According to our results, the most important source of variation of the *P-E* parameters in the area was depth, presumably as a result of covariation of depth with other variables such as irradiance. As a consequence of both the overall low values of α and the high covariation of $P^B_{m\ POC}$ and α (Fig. 4), the E_k values were rather high (mean of either 244 or 251 µmol photons m^{-2} s^{-1}, depending on the method of estimation), suggesting that phytoplankton assemblages were acclimated to high irradiance levels in the whole area. The absence of photoinhibition indicates that even the deeper cells could stand relatively high light intensities, implying that they had not been exposed to constantly low irradiances in their recent light history (Platt et al. 1980, Harding et al. 1987). This was the expected result if vertical mixing was sufficiently strong to bring these cells to shallow depths in a period short enough to prevent shade acclimation (Lewis et al. 1984, Cullen & Lewis 1988). In contrast, decreasing $P^B_{m\ POC}$ with depth is commonly interpreted as a result of shade acclimation (Falkowski 1981). Decreasing $P^B_{m\ POC}$ is frequently associated with increasing α (e.g. Dower & Lucas 1993, Basterretxea & Arístegui 2000, Morán et al. 2001), whereas both parameters decreased similarly with depth in our experiments (Fig. 5). Decreasing α with depth could be due to the packaging of pigments inside the chloroplasts (Sakshaug et al. 1997) or might reflect a parallel decrease in the C:chl *a* ratio (Geider et al. 1996, Taylor et al. 1997, Marañón & Holligan 1999), thus yielding no significant differences between surface and deep photosynthetic parameters if they were normalized to carbon instead of to chl *a*. In that case, however, it would be difficult to explain why the vertical mixing would be strong enough to avoid photoacclimation of P^B_m and α values, but not to prevent differences in the C:chl *a* ratio. An alternative explanation for the observed pattern could be related to temporal variability of hydrological features. Differential rates of change of physiological components in response to changes in irradiance could be expected (Lewis et al. 1984) if a different vertical light regime was being established due to a change in the physical conditions of the water column (i.e. due to increased stratification). Geider (1993) showed for instance that P^B_m and α respond differently, on a time basis, to changing irradiances. The slightly higher covariance with depth of $P^B_{m\ POC}$ ($r = 0.66$; $p < 0.001$) compared with that of α ($r = 0.53$; $p = 0.001$) or E_k ($r = 0.41$; $p = 0.017$) could perhaps be reflecting differential rates of response of the photosynthetic parameters considered.

Particulate and dissolved primary production

A clear relationship between irradiance and PER was identified, with consistently higher PER_E at lower irradiances for the whole data set (Figs. 7 & 8). The high PER_E values at low irradiances were not due to an absolute increase in DOC release rates, but to a sharp decrease in POC production with decreasing irradiance. These results suggest that a more or less constant amount of photosynthesized organic carbon was being lost from the algae independently of irradiance (within the experimental range used). PER enhancement under low irradiances is in agreement with previous reports obtained with more reduced data sets (Berman & Holm-Hansen 1974, Mague et al. 1980, Zlotnik & Dubinsky 1989, but see Verity 1981 for an exception). Despite considerable scatter, our PER_E values (Fig. 8) were considerably higher than those found by Zlotnik & Dubinsky (1989), who reported PERs <15% under almost all experimental irradiances with 3 algal cultures. At each experiment, we subtracted dark bottle values from those of the light bottles. Therefore, we do not think that these higher percentages were due to dark fixation of $^{14}CO_2$ as suggested by Watanabe (1980) and Fogg (1983). If the PER-irradiance relationship found here with natural assemblages happens to be general, incubations under suboptimal irradiance levels (i.e. lower than the corresponding E_k values) could result in PERs well above the commonly accepted values of <20% (Baines & Pace 1991, Hansell & Carlson 1998).

Zlotnik & Dubinsky (1989) also observed an increase in PER with high irradiances and it has been shown that one consequence of high irradiances, besides photoinhibition and lowering P^B values in the *P-E* relation-

ships, is an enhanced release into the environment of organic compounds such as glycolate (Leboulanger et al. 1997), as an alternative mechanism to photorespiration (Verity 1981, Wood & Van Valen 1990). In our case, high PER_E with high irradiances was observed at only some of the deep water experiments (Fig. 8B). This lack of generality may be partially explained by the absence of photoinhibition and the fact that, despite a trend of lower E_k values with depth, they were generally high in our samples.

The simultaneous measurement in the *P-E* experiments of TOC, POC and DOC production allowed a comparison of the differences in the calculated photosynthetic parameters for the total primary production and its particulate and dissolved fractions. With all data, $P^B_{m\ TOC}$ values were on average 19% higher than $P^B_{m\ POC}$, whereas differences were not significant for α and only marginally significant for E_k. As emphasized in Sakshaug et al. (1997), all photosynthesized organic carbon is part of the primary production so that, ideally, both the particulate and the dissolved fractions should be measured, although this is seldom attempted. We tentatively estimated a potential light-saturated chl *a*-normalized DOC production rate ($P^B_{m\ DOC}$) as the difference between fitted $P^B_{m\ TOC}$ and $P^B_{m\ POC}$ values. The relative contribution of this $P^B_{m\ DOC}$ to total primary production rate (PER_m) showed an increasing trend with depth when data from the 3 stations were pooled. Higher PER at depth was first reported by Thomas (1971) and Berman & Holm-Hansen (1974), who attributed it to the presence of senescent or light-limited cells. In our case, phytoplankton from below the upper mixed layer was effectively light-limited, i.e. experienced irradiances which were lower than their respective E_k values. Thus, the covariance of PER_m and depth could be related to the stronger effect of light limitation on POC than on DOC production as argued above.

Integrated primary production

Although differences among procedures in the estimates of PP_{int} were not very marked (Table 4), we regard the results of procedure no. 2, using interpolation of photosynthetic parameters at each depth, as more appropriate than just taking 2 sets of constant values changed at a given depth of the water column. Apart from the observation that Z_{uml} was shallower than the depth of the most superficial sample at Stns C2, A3 and B3 (Table 1), the fact that *P-E* parameters also varied with depth within the upper mixed layer, argued against the use of the uppermost values throughout all the upper mixed layer (Dower & Lucas 1993).

Average PP_{int} in this study was comparable to the data reported for frontal areas of the Alboran Sea or neighbouring Mediterranean regions (Sournia 1973, Estrada 1981, Lohrenz et al. 1988a,b, Estrada et al. 1993, Videau et al. 1994, Morán et al. 2001), but it showed a very high variability for both total and particulate values (Table 4) on a scale of 2 wk. The range of variation of PP_{int} across the Western Alboran Gyre (ca 23 for $PP_{int\ POC}$ and ca 35 for $PP_{int\ TOC}$) was high when compared to other parts of the Mediterranean on broader spatial and temporal scales (e.g. Sournia 1973, Lohrenz et al. 1988a,b, Estrada et al. 1993). Part of this variability was obviously due to changes in daily irradiance, but even using the average daily value obtained during the cruise, PP_{int} still varied by a factor of ca 6 (POC) and ca 9 (TOC). This high variability agrees with the conclusions of Côté & Platt (1983) concerning the difficulties of predicting short-term variations in primary productivity. In spite of this variability, an expected gradient of decreasing PP_{int} when moving away from the coastal upwelling zone towards the center of the gyre could be identified.

Our results stress the marked effect that variations in the light profile may have in the estimation of PP_{int}. At Stns A and C, considerable discrepancies in the estimated PP_{int} were obtained by sampling in the morning (Stns A4, C4) or in the afternoon (Stns A4b, C4b), with afternoon values being ca 70 and 200% higher, respectively (Table 4). Changes in the chl a_{int} values (15% increase at Stn A and the same value at Stn C) or the *P-E* parameters (practically the same except for α at Stn C) did not account for all that difference. Nevertheless, a 15 to 20 m shallowing of the peak of chl *a* at both stations (Fig. 11), perhaps caused by an internal wave, increased available PAR at the depth of maximum biomass from 0.4% of the surface value to 8% at Stn A, and from 6 to 21% at Stn C, hence leading to higher *in situ* estimates of primary production. Thus, short-term changes in available light for phytoplankton due to physical forcing would appear as a critical factor, neglected by logistic reasons in the conventional methods of calculating integrated rates of primary production. Although incident irradiance and vertical variability of phytoplankton biomass appear to play a relatively minor role in large data sets (Behrenfeld & Falkowski 1997b), underwater light distribution should be carefully considered when computing primary production estimates in locations showing subsurface chlorophyll maxima. Another source of variability, not considered here, is the effect of the vertical changes in the spectral composition of light (Platt & Sathyendranath 1988).

Although an overall significant relationship existed between surface and integrated values of chl *a* for all stations, PP_{int} showed no significant correlation with in-

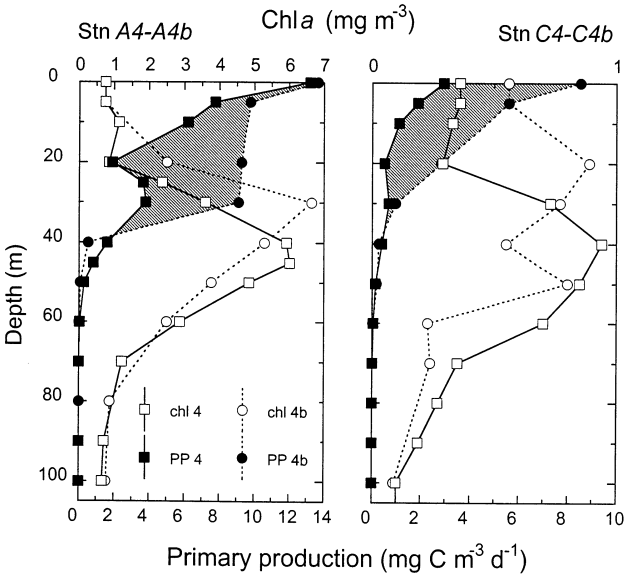

Fig. 11. Distribution of chl *a* and particulate primary production rates for the morning and afternoon samplings at Stns A4 and C4. Note the different scales. The shaded area represents the increase in estimated primary production from morning to afternoon

tegrated chl *a*. This can be explained by severe light limitation and low contribution to integrated primary production of the phytoplankton cells found at subsurface depths, which contained an important proportion of the total chl *a* in the water column. On the contrary, $PP_{int\ TOC}$ and $PP_{int\ POC}$ were significantly correlated to chl *a* at 5 m (Fig. 9), due to the high contribution to total primary production of surface or near-surface phytoplankton cells (Fig. 10). This finding is relevant for the estimation of regional primary production based on remote sensing, especially if it proves to hold true for all periods of the year. In some cases, the development of appropriate algorithms relating near-surface colour from satellite images (SeaWiFs, and formerly CZCS) and primary productivity has been based on good knowledge of the chl *a* distribution with depth (Longhurst et al. 1995, Sathyendranath et al. 1995). The lack of coupling between integrated chl *a* and primary production suggests that, in our study area, it would be more cost-effective to put more effort into determining the variability of surface chl *a* distributions.

Water column integrated PER values (PER_{int}, Table 4) were lower at Stn A3 (4%) than at Stns B3 or C3 (13 and 11%, respectively), which were outside of the influence of the phytoplankton bloom found at Stn A. However, the highest PER value (44%) was measured at Stn A2, which also presented the highest primary production. These contrasting results could be reflecting shifts in the composition and successional stage of the phytoplankton community. An alternative explanation for the higher PER found at this station would be, as observed by Fernández et al. (1994), a stronger dependence of bacterioplankton on phytoplankton-produced DOC at the less productive stations, which would result in artificially low PER because of bacterial consumption in the incubation bottles. As discussed above, the measurement of net $DO^{14}C$ concentration in the water at the end of the incubation period does not give any hint on its possible uptake by heterotrophic bacteria.

The appreciable variability in the *P-E* relationships found in a small area of the Alboran Sea, a likely consequence of a complex interaction of physical, chemical and biological factors in a highly hydrodynamical region, emphasizes the necessity of a spatially and temporally more detailed assessment of phytoplankton photophysiology (Platt et al. 1991, Behrenfeld & Falkowski 1997a, Sakshaug et al. 1997) to improve global ocean productivity models. The regular measurement of dissolved primary production in *P-E* experiments and the subsequent inclusion of the relevant parameters in productivity models would improve our understanding of the dynamics of marine DOC, a pool of crucial importance in the carbon cycle considered from a biogeochemical perspective.

Acknowledgements. We thank the people on board the RV 'Hespérides' for their help during the cruise. Mikel Latasa and Belén Martín-Míguez provided helpful comments on the manuscript. X.A.G.M. acknowledges the receipt of a *Formación de Personal Investigador* predoctoral fellowship from the Spanish Ministry of Education and Culture. This research was supported by grant MAS3-CT96-0051.

LITERATURE CITED

Amon RMW, Benner R (1994) Rapid cycling of high-molecular-weight dissolved organic matter in the ocean. Nature 369:549–552

Baines SB, Pace ML (1991) The production of dissolved organic matter by phytoplankton and its importance to bacteria: patterns across marine and freshwater systems. Limnol Oceanogr 36:1078–1090

Basterretxea G, Arístegui J (2000) Mesoscale variability in phytoplankton biomass distribution and photosynthetic parameters in the Canary-NW African coastal transition zone. Mar Ecol Prog Ser 197:27–40

Behrenfeld MJ, Falkowski PG (1997a) Photosynthetic rates derived from satellite-based chlorophyll concentration. Limnol Oceanogr 42:1–20

Behrenfeld MJ, Falkowski PG (1997b) A consumer's guide to phytoplankton primary productivity models. Limnol Oceanogr 42:1479–1491

Berman T, Holm-Hansen O (1974) Release of photoassimilated carbon as dissolved organic matter by marine phytoplankton. Mar Biol 28:305–310

Biddanda B, Benner R (1997) Carbon, nitogen, and carbohydrate fluxes during the production of particulate and dissolved organic matter by marine phytoplankton. Limnol Oceanogr 42:506–518

Cleveland JS, Perry MJ, Kiefer DA, Talbot MC (1989) Maximal quantum yield of photosynthesis in the northwestern Sargasso Sea. J Mar Syst 47:869–886
Coste B, Le Corre P, Minas HJ (1988) Re-evaluation of the nutrient exchanges in the Strait of Gibraltar. Deep-Sea Res 35:767–775
Côté B, Platt T (1983) Day-to-day variations in the spring-summer photosynthetic parameters of coastal marine phytoplankton. Limnol Oceanogr 28:320–344
Coveney MF (1982) Bacterial uptake of photosynthetic carbon from freshwater phytoplankton. Oikos 38:8–20
Cullen JJ, Lewis MR (1988) The kinetics of photoadaptation in the context of vertical mixing. J Plankton Res 10: 1039–1063
Dower KM, Lucas MI (1993) Photosynthesis-irradiance relationships and production associated with a warm-core ring shed from the Agulhas Retroflection south of Africa. Mar Ecol Prog Ser 95:141–154
Estrada M (1981) Biomasa fitoplanctónica y producción primaria en el Mediterráneo Occidental, a principios de otoño. Invest Pesq 45:211–230
Estrada M, Marrasé C, Latasa M, Berdalet E, Delgado M, Riera T (1993) Variability of deep chlorophyll maximum characteristics in the Northwestern Mediterranean. Mar Ecol Prog Ser 92:289–300
Falkowski PG (1981) Light-shade adaptation and assimilation numbers. J Plankton Res 3:203–216
Fernández M, Bianchi M, Van Wambeke F (1994) Bacterial biomass, heterotrophic production and utilization of dissolved organic matter photosynthetically produced in the Almeria-Oran front. J Mar Syst 5:313–325
Fogg GE (1983) The ecological significance of extracellular products of phytoplankton photosynthesis. Bot Mar 26: 3–14
Geider RJ (1993) Quantitative phytoplankton physiology: implications for primary production and phytoplankton growth. ICES Mar Sci Symp 197:52–62
Geider RJ, MacIntyre HL, Kana TM (1996) A dynamic model of photoadaptation in phytoplankton. Limnol Oceanogr 41:1–15
Gómez F, Echevarría F, García CM, Prieto L, Ruiz J, Reul A, Jiménez-Gómez F, Varela M (2000) Microplankton distribution in the Strait of Gibraltar: coupling between organisms and hydrodynamic structures. J Plankton Res 22: 603–617
Hansell DA, Carlson CA (1998) Net community production of dissolved organic carbon. Global Biogeochem Cycles 12: 443–453
Harding LW Jr, Fisher TR Jr, Tyler MA (1987) Adaptive responses of photosynthesis in phytoplankton: specificity to time-scale of change in light. Biol Oceanogr 4:403–437
Heburn GW, La Violette PE (1990) Variations in the structure of the anticyclonic gyres found in the Alboran Sea. J Geophys Res 95:1599–1613
Hood RR (1995) Light response of phytoplankton in the South Atlantic Ocean: interpretation of observations and application to remote sensing. J Geophys Res 100:10927–10942
Jiménez F, Rodríguez J, Bautista B, Rodríguez V (1987) Relations between chlorophyll, phytoplankton cell abundance and biovolume during a winter bloom in Mediterranean coastal waters. J Exp Mar Biol Ecol 105:161–173
Kyewalyanga MN, Platt T, Sathyendranath S, Lutz VA, Stuart V (1998) Seasonal variations in physiological parameters of phytoplankton across the North Atlantic. J Plankton Res 20:17–42
Lancelot C (1979) Gross excretion rates of natural marine phytoplankton and heterotrophic uptake of excreted products in the southern North Sea, as determined by short-term kinetics. Mar Ecol Prog Ser 1:179–186
Leboulanger C, Oriol L, Jupin H, Descolas-Gros C (1997) Diel variability of glycolate in the eastern tropical Atlantic Ocean. Deep-Sea Res 44:2131–2139
Lewis MR, Cullen JJ, Platt T (1984) Relationships between vertical mixing and photoadaptation of phytoplankton: similarity criteria. Mar Ecol Prog Ser 15:141–149
Lohrenz SE, Arnone RA, Wiesenburg DA, DePalma I (1988a) Satellite detection of transient enhanced primary production in the western Mediterranean Sea. Nature 335: 245–247
Lohrenz SE, Wiesenburg DA, DePalma IP, Johnson KS, Gustafson DE (1988b) Interrelationships among primary production, chlorophyll, and environmental conditions in frontal regions of the western Mediterranean Sea. Deep-Sea Res 35:793–810
Longhurst A, Sathyendranath S, Platt T, Caverhill C (1995) An estimate of global primary production in the ocean from satellite radiometer data. J Plankton Res 17:1245–1271
Mague TH, Friberg E, Hughes DJ, Morris I (1980) Extracellular release of carbon by marine phytoplankton: a physiological approach. Limnol Oceanogr 25:262–279
Marañón E, Holligan PM (1999) Photosynthetic parameters of phytoplankton from 50° N to 50° S in the Atlantic Ocean. Mar Ecol Prog Ser 176:191–203
Minas HJ, Coste B, Le Corre P, Minas M, Raimbault P (1991) Biological and geochemical signatures associated with the water circulation through the Strait of Gibraltar and in the western Alboran Sea. J Geophys Res 96:8755–8771
Mitchell BG, Holm-Hansen O (1991) Observations and modelling of the Antarctic phytoplankton crop in relation to mixing depth. Deep-Sea Res 38:981–1007
Morán XAG, Taupier-Letage I, Vázquez-Domínguez E, Ruiz S, Arin L, Raimbault P, Estrada M (2001) Physical-biological coupling in the Algerian Basin (SW Mediterranean): influence of mesoscale instabilities on the biomass and production of phytoplankton and bacterioplankton. Deep-Sea Res 48:405–437
Morán XAG, Gasol JM, Pedrós-Alió C, Estrada M (in press) Dissolved and particulate primary production and bacterial production in offshore Antarctic waters during austral summer: coupled or uncoupled? Mar Ecol Prog Ser
Nagata T (2000) Production mechanisms of dissolved organic matter. In: Kirchman DL (ed) Microbial ecology of the oceans. John Wiley & Sons, New York, p 121–152
Norrman B, Zweifel UL, Hopkinson CS Jr, Fry B (1995) Production and utilization of dissolved organic carbon during an experimental diatom bloom. Limnol Oceanogr 40: 898–907
Packard TT, Minas HJ, Coste B, Martinez R, Bonin MC, Gostan J, Garfield P, Christensen J, Dortch Q, Minas M, Copin-Montegut G, Copin-Montegut C (1988) Formation of the Alboran oxygen minimum zone. Deep-Sea Res 35: 1111–1118
Perkins H, Kinder T, La Violette P (1990) The Atlantic inflow in the western Alboran Sea. J Phys Oceanogr 20:242–263
Platt T (1985) Phytoplankton production in oligotrophic marine ecosystems: the Mediterranean Sea. In: Moraitou-Apostolopoulou M, Kiortsis V (eds) Mediterranean marine ecosystems. Plenum Press, New York, p 231–246
Platt T, Sathyendranath S (1988) Oceanic primary production: estimation by remote sensing at local and regional scales. Science 241:1613–1620
Platt T, Gallegos CL, Harrison WG (1980) Photoinhibition of photosynthesis in natural assemblages of marine phytoplankton. J Mar Res 38:687–701

Platt T, Caverhill C, Sathyendranath S (1991) Basin-scale estimates of oceanic primary production by remote sensing: the North Atlantic. J Geophys Res 96:15147–15159

Rodríguez V (Rapporteur), Bautista B, Blanco JM, Figueroa FL, Cano N, Ruiz J (1994) Hydrological structure, optical characteristics and size distribution of pigments and particles at a frontal station in the Alboran Sea. Working Group 1 Report. Sci Mar 58:31–41

Rodríguez J, Blanco JM, Jiménez-Gómez F, Echevarría F, Gil J, Rodríguez V, Ruiz J, Bautista B, Guerrero F (1998) Patterns in the size structure of the phytoplankton community in the deep fluorescence maximum of the Alboran Sea (southwestern Mediterranean). Deep-Sea Res 45: 1577–1593

Sakshaug E, Bricaud A, Dandonneau Y, Falkowski PG, Kiefer DA, Legendre L, Morel A, Parslow J, Takahashi M (1997) Parameters of photosynthesis: definitions, theory and interpretation of results. J Plankton Res 19:1637–1670

Sathyendranath S, Longhurst AR, Caverhill CM, Platt T (1995) Regionally and seasonally differentiated primary production in the North Atlantic. Deep-Sea Res 42: 1773–1802

Sournia A (1973) La production primaire planctonique en Méditerranée: essai de mise à jour. Bull Étude en Commun Méditerr 5:1–128

Taylor AH, Geider RJ, Gilbert FJH (1997) Seasonal and latitudinal dependencies of phytoplankton carbon-to-chlorophyll ratios: results of a modelling study. Mar Ecol Prog Ser 152:51–66

Thomas JP (1971) Release of dissolved organic matter from natural populations of marine phytoplankton. Mar Biol 11: 311–323

Tintoré J, Gomis D, Alonso S, Parrilla G (1991) Mesoscale dynamics and vertical motion in the Alborán Sea. J Phys Oceanogr 21:811–823

Verity P (1981) Effects of temperature, irradiance, and daylength on the marine diatom *Leptocylindrus danicus* Cleve. II. Excretion. J Exp Mar Biol Ecol 55:159–169

Videau C, Sournia A, Prieur L, Fiala M (1994) Phytoplankton and primary production characteristics at selected sites in the geostrophic Almeria-Oran front system (SW Mediterranean Sea). J Mar Syst 5:235–250

Watanabe Y (1980) A study of the excretion and extracellular products of natural phytoplankton in Lake Nakanuma, Japan. Int Rev Ges Hydrobiol 65:809–834

Webb WL, Newton M, Starr D (1974) Carbon dioxide exchange of *Alnus rubra*: a mathematical model. Oecologia 17:281–291

Williams PJleB (1993) Chemical and tracer methods of measuring plankton production. ICES Mar Sci Symp 197: 20–36

Williams PJleB, Robinson C, Søndergaard M, Jespersen AM, Bentley TL, Lefèvre D, Richardson K, Riemann B (1996) Algal ^{14}C carbon and total carbon metabolisms. 2. Experimental observations with the diatom *Skeletonema costatum.* J Plankton Res 18:1961–1974

Wood AM, Van Valen LM (1990) Paradox lost? On the release of energy-rich compounds by phytoplankton. Mar Microb Food Webs 4:103–116

Yentsch CS, Menzel DW (1963) A method for the determination of phytoplankton chlorophyll and phaeophytin by fluorescence. Deep-Sea Res 10:221–231

Zlotnik I, Dubinsky Z (1989) The effect of light and temperature on DOC excretion by phytoplankton. Limnol Oceanogr 34:831–839

Editorial responsibility: Otto Kinne (Editor), Oldendorf/Luhe, Germany

Submitted: February 21, 2000; Accepted: August 9, 2000
Proofs received from author(s): February 19, 2001